microbial biotechnology

Open Access

Ammonia threshold for inhibition of anaerobic digestion of thin stillage and the importance of organic loading rate

Jan Moestedt,[1,2]* Bettina Müller,[2] Maria Westerholm[2] and Anna Schnürer[2]

[1]*Department of Biogas R&D, Tekniska verken i Linköping AB, Box 1500, Linköping SE-581 15, Sweden.*

[2]*Department of Microbiology, BioCenter, Swedish University of Agricultural Sciences, Box 7025, Uppsala SE-750 07, Sweden.*

Summary

Biogas production from nitrogen-rich feedstock results in release of ammonia (NH_3), causing inhibition of the microbial process. The reported threshold ammonia value for stable biogas production varies greatly between studies, probably because of differences in operating conditions. Moreover, it is often difficult to separate the effect of ammonia inhibition from that of organic loading rate (OLR), as these two factors are often interrelated. This study attempted to distinguish the effects of ammonia and OLR by analysis of two laboratory-scale biogas reactors operating with thin stillage and subjected to an increase in free ammonia (from 0.30 to 1.1 g L^{-1}) either by addition of an external nitrogen source (urea) or by increasing the OLR (3.2–6.0 g volatile solids L^{-1} d^{-1}). The results showed that ammonia concentration was detrimental for process performance, with the threshold for stability in both processes identified as being about 1 g NH3-N L^{-1}, irrespective of OLR. Analysis of the methanogenic community showed limited differences between the two reactors on order level and a clear increase in the abundance of *Methanomicrobiales*, particularly *Methanoculleus* sp., in response to increasing ammonia concentration. Further comprehensive molecular analysis revealed that diverse *Methanoculleus* species dominated in the reactors at a given ammonia level at different OLR. The acetogenic community was clearly affected by both ammonia concentration and OLR, suggesting that the volatile fatty acid load in relation to the higher OLR was important for the dynamics of this community.

Received 16 January, 2015; revised 24 September, 2015; accepted 27 September, 2015. *For correspondence. E-mail: jan.moestedt@tekniskaverken.se; Tel. +46 13 20 93 77; Fax +46 13 20 80 06.
Microbial Biotechnology (2016) **9**(2), 180–194
doi:10.1111/1751-7915.12330
Funding Information This project was funded by Tekniska verken i Linköping AB (publ.) and the Swedish Research Council Formas, and formed part of the thematic research programme MicroDrivE at the Swedish University of Agricultural Sciences.

Introduction

Biogas formation from organic material proceeds through an array of reactions and requires a complex microbial community performing different interacting metabolic actions. This anaerobic degradation can be divided into four main steps; hydrolysis, acidogenesis, acetogenesis and methanogenesis (Angelidaki *et al.*, 2011). During hydrolysis, extracellular enzymes disintegrate complex macromolecules into monomers such as amino acids, fatty acids and sugars. These compounds are used during acidogenesis by fermentative bacteria, and the main products are volatile fatty acids, alcohols, hydrogen and carbon dioxide. During acetogenesis, the longer fatty acids are converted into acetate and hydrogen/carbon dioxide by different syntrophic oxidation reactions. Finally, acetate and hydrogen/carbon dioxide are converted to methane and carbon dioxide by acetotrophic and hydrogenotrophic methanogens respectively (Zinder, 1984). Alternatively, acetate may be oxidized to carbon dioxide and hydrogen by syntrophic acetate oxidation (SAO) coupled with hydrogenotrophic methanogenesis (Zinder and Koch, 1984; Schnürer *et al.*, 1999). The different degradation steps proceed in a synchronized manner and decreased activity of one or several microbial groups can severely affect the efficiency and even lead to process failure.

Protein-rich materials have high bio-methane potential (BMP) and are thus interesting materials for commercial biogas production (Ek *et al.*, 2011; Nordell *et al.*, 2013). Unfortunately, high loads of such materials are often correlated with process instability due to the release of ammonia nitrogen (NH_3-N) (Chen *et al.*, 2008; Rajagopal *et al.*, 2013; Yenigün and Demirel, 2013), causing inhibition of the microbial degradation process. Ammonia is released from degradation of amino acids during acidogenesis, and at elevated concentrations it is toxic for different microorganisms, in particular methanogens (Chen *et al.*, 2008). The free ammonia nitrogen (FAN) level resulting in inhibition varies, but in both pure cultures and different reactors acetotrophic methanogens have

been shown to be more sensitive to elevated FAN levels than hydrogenotropic methanogens (Koster and Lettinga, 1984; Sprott and Patel, 1986; Angelidaki and Ahring, 1993; Hansen *et al*., 1998a). As a consequence of this, SAO processes involving ammonia-tolerant species have been shown to develop at elevated FAN levels (Westerholm *et al*., 2012; Werner *et al*., 2014). Despite inhibition of acetotrophic methanogens relatively stable operation is thus possible but commonly with reduced methane yield (Schnürer and Nordberg, 2008; Westerholm *et al*., 2012).

For commercial biogas production, it is important to maximize the methane yield, and this is typically achieved by increasing the organic load. In the case of protein-rich materials, for example thin stillage, this practice can result in very high FAN concentrations, particularly if the feedstock is concentrated in order to maintain long hydraulic retention time (HRT). Biogas plant operators then need to monitor for indications of ammonia inhibition in order to avoid process failure. In such conditions, it can be problematic to separate the effect of increasing FAN from that occurring due to higher load of organic material. These two factors are interlinked, making it difficult to achieve optimal management conditions, particularly as the maximum FAN concentration for steady, efficient anaerobic digestion processes remains somewhat unclear.

The aim of this study was thus to investigate the NH_3-N inhibition threshold concentration in a biogas system treating protein-rich thin stillage, where methane formation mainly proceeded via SAO. The study was conducted in two laboratory-scale biogas reactors subjected to an increase in ammonia (0.30–1.1 g L^{-1}). The effect of organic loading rate (OLR) was discriminated from that of ammonia concentration by using an increase in the organic load to increase the ammonia concentration in one reactor (R_{OLR}) and by adding urea to the other reactor (R_{UREA}). Process performance was monitored through analyses of chemical and microbiological parameters.

Results and discussion

Reactor performance

The inoculum used in the experiment was obtained from a well-studied biogas plant (Moestedt *et al*., 2013a,b; Sun *et al*., 2014), treating thin stillage as the main substrate, with an average FAN concentration of about 0.3 g L^{-1} and with steady biogas production for several years. Tracer analysis in previous studies of this biogas plant have confirmed dominance of SAO for acetate degradation (Moestedt *et al*., 2013b; Sun *et al*., 2014). During the start-up phase (days 1–100), reactors R_{UREA} and R_{OLR} showed similar performance regarding biogas and methane yield as well as levels of ammonia and volatile fatty acid (VFA): 0.32 ± 0.02 L CH_4 g^{-1} volatile solids (VS), 54.3 ± 0.02% CH_4, 0.35 g FAN L^{-1}, 1.3 ± 0.9 g Tot-VFA L^{-1} for R_{UREA} and 0.31 ± 0.02 L CH_4 g^{-1} VS, 53.4 ± 0.02 % CH_4, 0.35 g FAN L^{-1}, 0.8 ± 0.4 g Tot-VFA L^{-1} for R_{OLR} (Figs 1 and 2). The degree of degradation (on VS basis) was also similar after 100 days with 76 ± 8% and 78 ± 11 % in R_{UREA} and R_{OLR} respectively. The obtained methane yield in the reactors was in line with a previous analysis of the thin stillage, showing a maximum BMP of 0.32 L CH_4 g^{-1} VS (Moestedt, 2015). The overall performance of the reactors was also similar to those in the commercial biogas plant from which inoculum and substrates were collected, thus indicating a successful start-up phase, possible to use as a reference period in the study.

From day 100 to day 313, the FAN concentration gradually increased in both reactors from 0.30 to 0.65 g L^{-1} as a result of increasing OLR in R_{OLR} and urea addition in

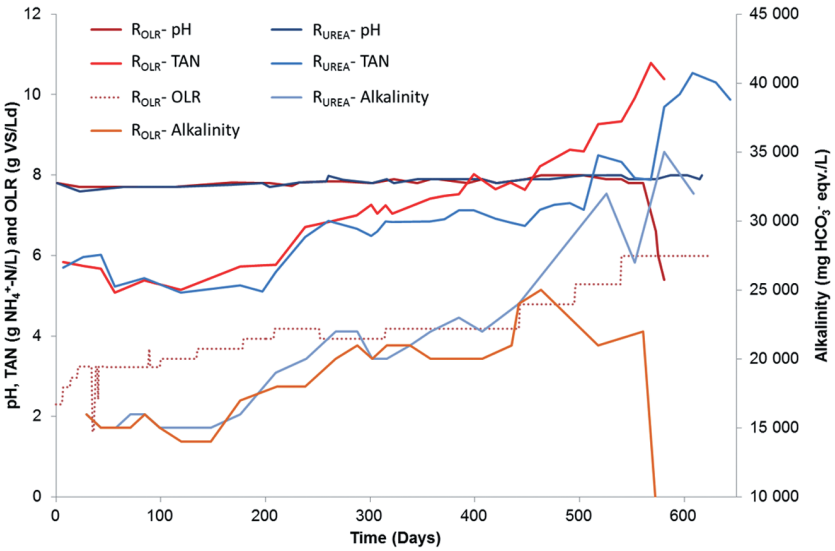

Fig. 1. pH, alkalinity and TAN in reactors R_{UREA} and R_{OLR}. In addition, OLR is given for R_{OLR}. Organic loading rate for R_{UREA} is not shown but was identical to that for R_{OLR} until day 100, and thereafter remained constant at 3.2 g VS L^{-1} day^{-1}.

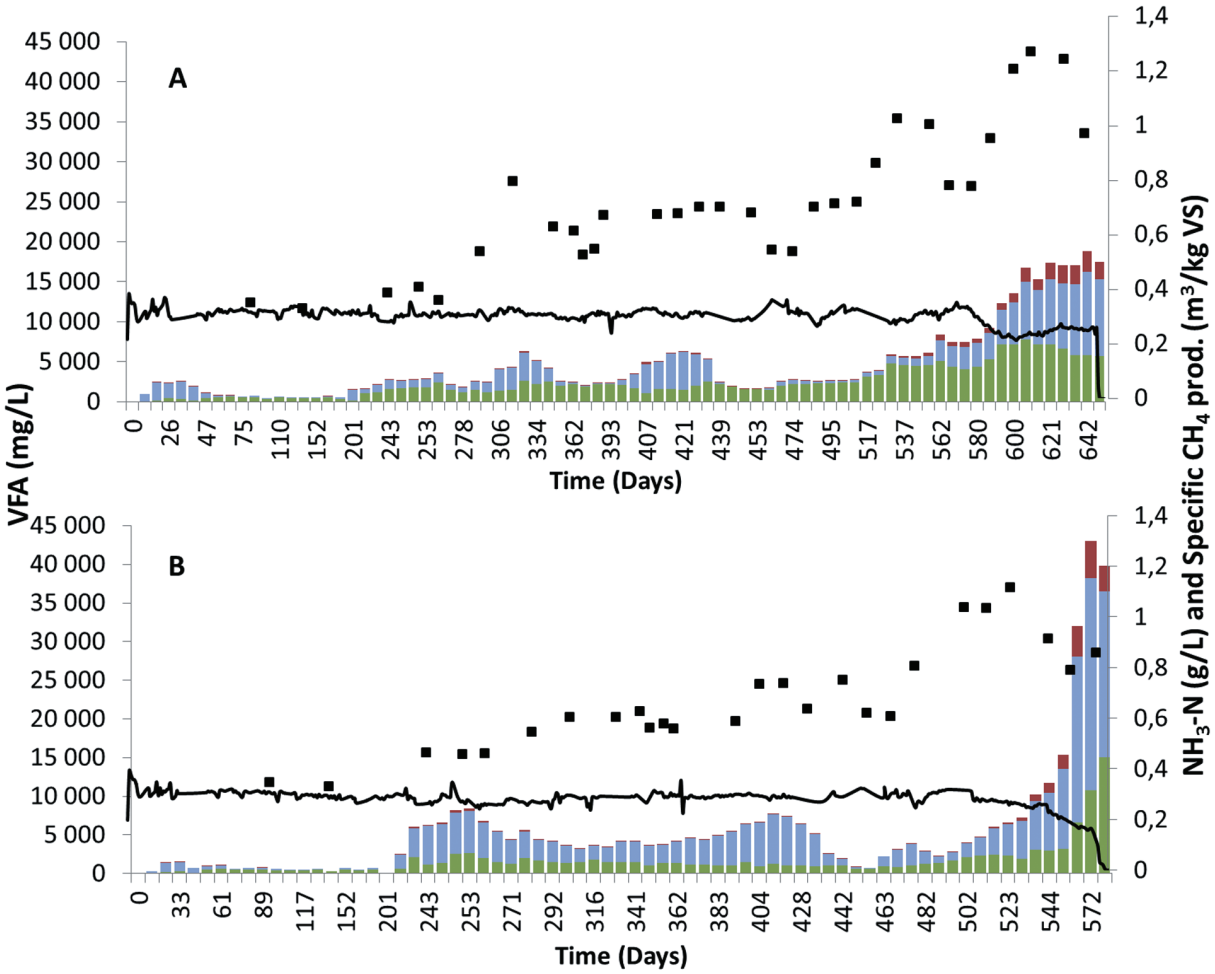

Fig. 2. Composition of (acetate ■, propionate ■, residual acids ■), specific methane gas production (—) and FAN concentration (-■-) in (A) reactor R_{UREA} and (B) reactor R_{OLR}.

R_{UREA}. On reaching 4.2 g VS L^{-1} d^{-1} and a FAN level of 0.46 g L^{-1}, which occurred at day 209, the level of VFA increased in R_{OLR}. Propionate increased in particular but acetate also accumulated, giving a total VFA concentration of 8.4 g L^{-1} (Fig. 2B). The FAN concentration (0.46 g L^{-1}) at that point was at a level previously reported to cause process instability in the reference full-scale biogas plant (Moestedt *et al.*, 2013b). However, by decreasing the organic load to 3.9 g VS L^{-1}·day and allowing time for microbial adaptation to the increasing FAN levels, it was possible to reduce the VFA level and achieve process recovery until day 442. During the period between days 100–313, the VFA concentration also increased in R_{UREA} to above 5 g L^{-1}, and therefore OLR and urea dose were kept constant between day 313 and day 442 to allow for microbiological adaptation. The total ammonia nitrogen (TAN) concentration in reactors R_{UREA} and R_{OLR} was 6.9 ± 0.13 g L^{-1} and 7.5 ± 0.3 g L^{-1}, respectively, and both reactors had FAN concentration of 0.65 ± 0.01 g L^{-1}, and the alkalinity in the reactors was 21–22 ± 1 g L^{-1}. The specific methane production was also comparable in the two reactors 0.31 ± 0.02 L and 0.29 ± 0.01 L CH_4 g^{-1} VS, for R_{UREA} and R_{OLR}, respectively, close to values from the start-up phase of the experiment. The pH remained constant during this period in either reactor, and the VFA concentration in R_{OLR} was on average 4.7 ± 0.7 g L^{-1}, with 73% consisting of propionate, while in R_{UREA} it was 3.8 ± 0.8 g L^{-1}, with 47% as propionate (Figs 1 and 2). The degree of degradation was high, 77 ± 2% and 77 ± 1% in R_{UREA} and R_{OLR} respectively.

After the adaptation period, the OLR/urea dose was again increased. In R_{OLR}, the OLR was increased in steps to 4.8 and 5.3 g VS L^{-1} day, finally reaching 6.0 g VS L^{-1} day at day 540. During the same period, the urea dose to R_{UREA} was adjusted to achieve a similar increase in FAN as in R_{OLR} (Table 1). This resulted in a FAN concentration of > 1 g L^{-1} after 500 days in R_{OLR} and 520 days in R_{UREA}

Table 1. Organic loading rate (gVS L^{-1} day^{-1}) of reactor R_{OLR} and urea dosage (g d^{-1}) of reactor R_{UREA}. The OLR of R_{UREA} was constant at 3.2 g VS L^{-1} d^{-1} from day 20. The urea dose was regulated according to the resulting FAN concentration in R_{OLR}, and thus the dosage varied somewhat throughout the operation.

Days	OLR (g VS L^{-1} day^{-1})	Urea dose (g day^{-1})
0–20	Increase from 2.3 to 3.2	–
21–99	3.2	–
100–134	3.4	0.11
135–178	3.7	0.24
179–208	3.9	0.37
209–251	4.2	0.61–1.2
252–314	3.9	0.48–0.70
315–442	4.2	0.83
443–495	4.8	1.2–1.7
496–539	5.3	1.6–2.3
540–	6.0	2.0–3.6

(Fig. 2). This high ammonia level caused a rapid increase in VFA in both reactors, followed by a decrease in pH and in specific methane production in the final phase of the process (Fig. 2). This clearly illustrates that the threshold concentration for maintained process stability had been reached.

The fact that the specific methane yield was maintained until the final phase of the experiment reflected successful adaptation of the microbial community to the increased FAN concentration. However, accumulation of VFA occurred periodically, requiring operation at a lower OLR (Fig. 2). Similarly, several previous studies have shown that adaptation of anaerobic digestion to high FAN is possible, most likely as a result of selection of ammonia-tolerant species. For example, Calli and colleagues (2005) observed process adaptation to FAN concentration above 0.80 g L^{-1} by increasing the level over a long period (450 days) in upflow anaerobic sludge blanket (UASB) reactors treating synthetic wastewater, but still with propionate accumulation of up to 0.5 g L^{-1} (50% of total VFA). In a study in thermophilic continuously stirred tank reactors (CSTR) reactors with HRT of 15 days treating manure, adaptation to reach a FAN concentration of 0.60–0.80 g L^{-1} proved possible, but with higher VFA levels (propionate concentration ~3.5 g L^{-1}) than in low-ammonia reference reactors (Angelidaki and Ahring, 1994). Another nitrogen adaptation experiment resulted in stable, but lower, methane yield and elevated total VFA concentration (up to 5 g L^{-1}) when the FAN concentration was increased from approximately 0.60 to 1.20 g L^{-1} (Angelidaki and Ahring, 1993). Furthermore, both mesophilic and thermophilic commercial-scale biogas plants (CSTR) have been reported to operate at high FAN levels (0.52–0.80 g L^{-1}) for several years with maintained process stability at HRT of 24–60 days (Sun *et al.*, 2014).

The process failure in reactors R_{UREA} and R_{OLR} at an almost identical FAN concentration (> 1 g L^{-1}) illustrated the low impact of OLR (which at this time was 88% higher than the starting value in R_{OLR}) on the critical FAN threshold. The FAN level resulting in process failure was in agreement with values reported previously for FAN-adapted processes operating at similar temperature and pH (Hansen *et al.*, 1998a; Lauterböck *et al.*, 2012). However, while process failure in the two reactors occurred at the same FAN level, the breakdown occurred faster in R_{OLR} and the VFA accumulation pattern differed somewhat (Fig. 2). Propionate was the dominant VFA during the whole experimental period in R_{OLR}, while in R_{UREA} acetate was the dominant acid up to a FAN level of > 1 g L^{-1}, above which the propionate concentration increased rapidly. The difference in VFA accumulation pattern between the reactors can probably be explained by increased throughput of VFAs following the higher OLR in R_{OLR}, resulting in higher stress for that microbial community. Since propionate increased in both reactors on reaching the threshold FAN level, it seems to be an indicator of FAN inhibition (Fig. 2), as suggested previously (Angelidaki and Ahring, 1993; Ahring *et al.*, 1995). The accumulation of propionate could have been caused either by inhibition of propionate-oxidizing bacteria or by the degradation in acidogenesis being directed towards more propionate production. Calli and colleagues (2005) reported reduced abundance of acetogenic bacteria in response to increasing FAN level and propionate formation and concluded that propionate formation was caused by inhibition of propionate oxidizers. On the other hand, FAN-inhibited methanogenesis results in higher hydrogen pressure, which in turn is correlated with a shift in acidogenesis from acetate, hydrogen and carbon dioxide towards production of longer acids (Worm *et al.*, 2010). This could also explain the increased production of propionate following higher OLR in reactor R_{OLR}.

Reactor R_{UREA} survived without complete process failure for 100 days longer than R_{OLR}, but with reduced gas yield compared with start-up (Fig. 2). The difference between the reactor can be explained by a pH variation (from pH 8.0 to 7.9) and a somewhat lower TAN in R_{UREA}, resulting in a reduction of the FAN concentration to 0.77 g L^{-1} due to a shift in equilibrium between NH_4^+ and NH_3 after reaching the FAN threshold. In the present case, the longer process survival in R_{UREA} despite the high VFA concentration could also be an effect of the very high alkalinity, as a result of the high amount of added urea. However, R_{UREA} eventually ceased to produce methane too, at FAN levels above 1.2 g L^{-1}.

Methanogenic community analysis

Quantitative polymerase chain reaction (qPCR) analyses of reactor liquid showed similar levels of hydrogenotrophic *Methanomicrobiales* and *Methanobacteriales* in both reactors (Fig. 3). No *Methanosaetae* or *Methanosarcina* were

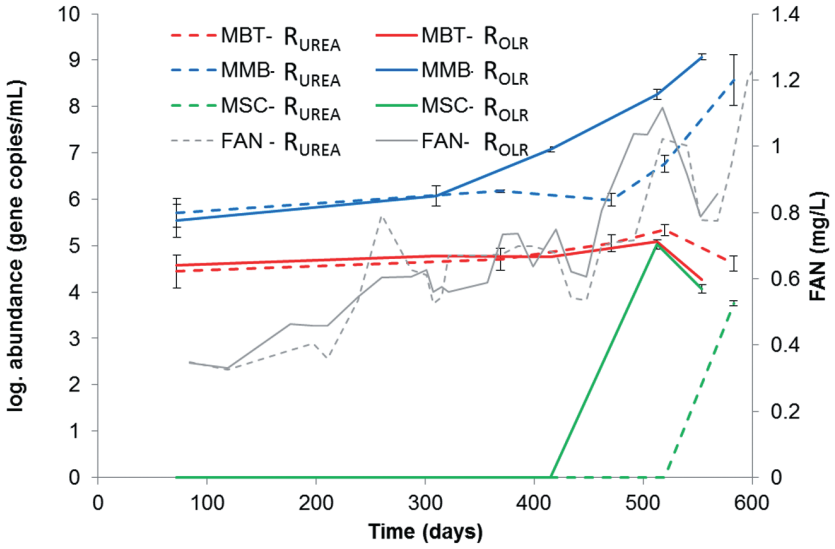

Fig. 3. Log abundance of methanogenic groups and free ammonia nitrogen (FAN) concentration in reactors R_{OLR} and R_{UREA} (dotted lines). *Methanobacteriales* (MBT), *Methanomicrobiales* (MMB), *Methanosarcinaceae* (MSC).

detected at start-up, as also reported for other SAO-dominated processes (Karakashev *et al.*, 2006; Sun *et al.*, 2014). The absence of *Methanosaetae* was expected due to its apparent sensitivity to high FAN (Sprott and Patel, 1986), as was the dominance of hydrogenotrophic methanogens, which are known to have higher tolerance (Hansen *et al.*, 1998a; Angenent *et al.*, 2002; Westerholm *et al.*, 2011a; Sun *et al.*, 2014). With increasing FAN concentration (from 0.30 g L^{-1} to > 1.0 g L^{-1}), the abundance of *Methanomicrobiales* increased in both reactors, from log 5.5–5.7 gene copies mL^{-1} during start-up to log 8.6–9.1 gene copies/ml at the end point, just before process failure occurred. The increase was statistically significant ($P = 0.001$ for R_{UREA}, $P = 0.0001$ for R_{OLR}; Student's *t*-test) (Fig. 3). The abundance of *Methanomicrobiales* increased somewhat earlier in R_{OLR} than in R_{UREA} (day 313 onward), which correlated with the earlier increase of FAN in R_{OLR} (Fig. 3). The increase of *Methanomicrobiales* in R_{UREA} was somewhat unexpected and shows that the higher substrate load was not the reasons for the higher abundance. As there was no increase in methane production at the end of the experiment one possible explanation might be that a population shift occurred within the *Methanomicrobiales* towards species harbouring multiple copies of the 16s RNA gene or expressing a less efficient methanogenic metabolism. The *mcrA* clone libraries obtained from start and end points indicate such a species change within the genus *Methanoculleus*, in which e.g. OTU1 is less abundant at the end point compared with e.g. OTU9, which abundance increased in both R_{UREA} and R_{OLR} (Fig. 4; Fig. 5).

Terminal restriction fragment length pattern (T-RFLP) analysis and subsequent clone library targeting the *mcrA* gene, in which R_{OLR} day 72 was assumed to represent the start-up phase in both reactors since they had been treated identically until then, showed corresponding results as found in the qPCR analysis, i.e. with higher FAN concentration the community was indeed dominated by increasing *Methanomicrobiales* (Fig. S1; Fig. 4). The 94 bp terminal restriction fragment (T-RF), which dominated during the whole operating period (70–77%), corresponded to the majority (75–90%) of recovered genotypes in the clone library. These genotypes are summarized as operational taxonomic unit (OTUs) 1, 7, 8 and 9, which were found to be identical or closely related to different *Methanoculleus* species (Fig. S1; Fig. 4). In accordance with the higher gene copy number for *Methanomicrobiales* obtained by qPCR, this T-RF also showed higher abundance in R_{OLR} at day 415 compared with R_{UREA} at day 471 (Fig. S1).

The most abundant genotype in the *mcrA* clone library was OTU1, representing 34–37% at the end point in both reactors. This OTU was > 96% identical to *Methanoculleus bourgensis* strain BA1. This genotype appeared at constant relative abundance from start-up to end point in both reactors and hence was apparently not affected by the increasing FAN and OLR (Fig. 5). Interestingly, except for this common genotype the clone libraries retrieved from end points showed differences in the *Methanoculleus* population structure between the reactors, specifically the relative abundance of OTU7 and OTU9 (Fig. 4; Fig. 5). Both these OTUs were recovered at higher frequency in R_{OLR}, together providing 35% of the methanogenic community recovered compared with 20% in R_{UREA}. Operational taxonomic unit 9 was 98% identical to *M. bourgensis* strain MAB2, while OTU7 was 91% similar to *Methanoculleus chikugoensis* (Fig. 4). In addition to these highly abundant OTUs, a rather small fraction of the end-point community (4–8%) was identified as the type strain *M. bourgensis* CB1 and the *M. bourgensis*

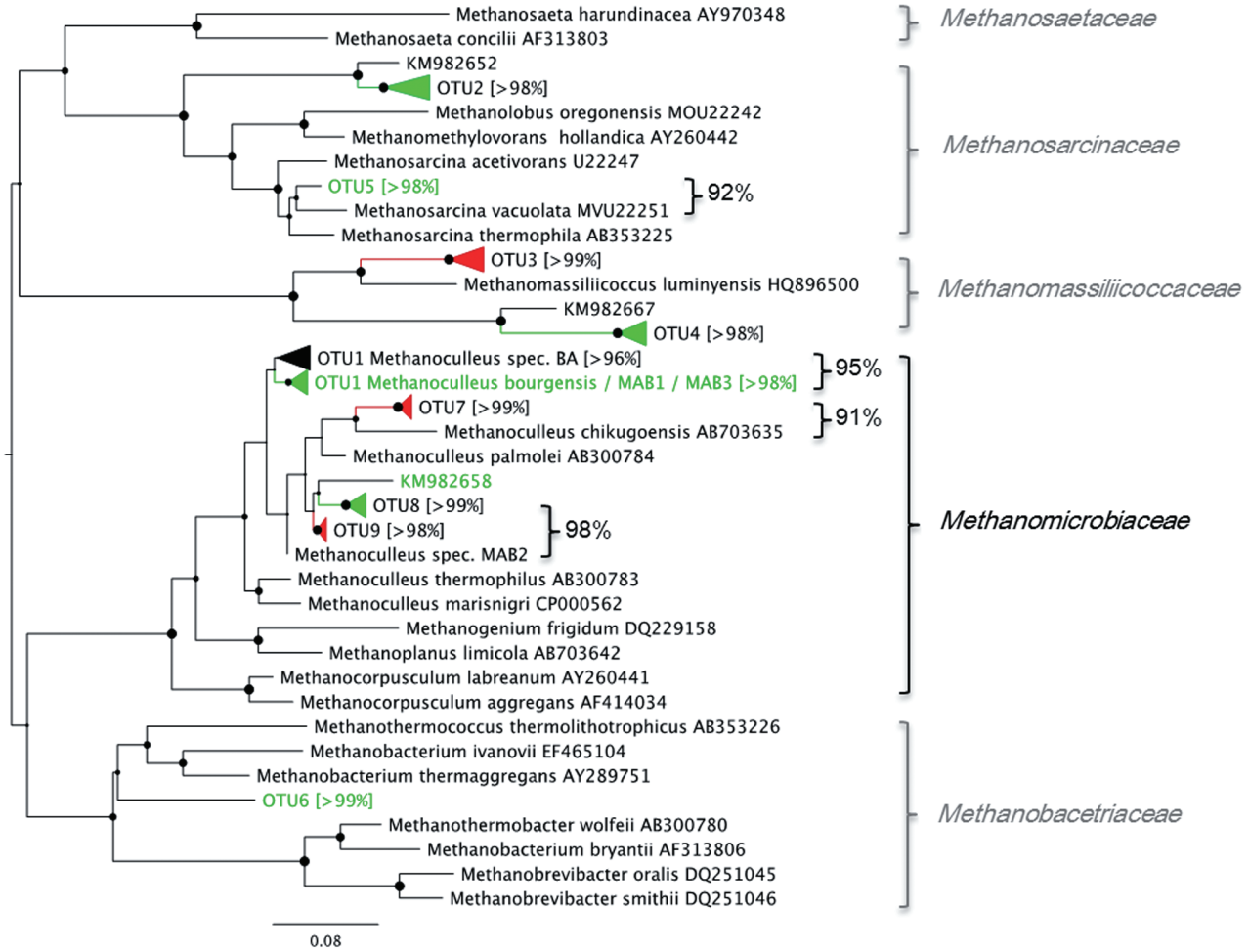

Fig. 4. Phylogenetic tree constructed of sequences retrieved in the clone library of the *mcrA* gene. Operational taxonomic units retrieved from three different samples (start-up and end point of each reactor), with theoretical T-RF sequence lengths indicated in brackets. Green font indicates dominance in R_{UREA} at end point, red indicates dominance in R_{OLR} at end point, and black indicates similar abundance in both reactors at end point or throughout the experiment. Sequence identity is given (%) for selected genotypes.

strains MAB1 and MAB3 (all defined as OTU1 with > 94.5% identity). The dominance of *Methanoculleus* species within *Methanomicrobiales* and the increased abundance of *Methanoculleus* sp. concurrently with the increase in FAN concentration appear typical for ammonia-dominated processes (Angenent *et al.*, 2002; Westerholm *et al.*, 2011a; 2012; Nikolausz *et al.*, 2013; Sun *et al.*, 2014). Moreover, several of the identified species have previously been found in high ammonia processes, i.e. *M. bourgensis* strain BA1, MAB1, MAB2 and MAB3 (Schnürer *et al.*, 1999) and tentatively also indicated for *M. chikugoensis* (Cardinali-Rezende *et al.*, 2012). This result further illustrates the high ammonia tolerance of these organisms and suggests an important role in SAO.

Methanosarcinaceae and *Methanobacteriales* were not retrieved in the clone libraries and did not appear in the T-RFLP from R_{OLR}. The qPCR analyses showed low or not detectable levels of these species in both reactors, indicating low impact of these species on the methanogenesis in these processes. In R_{UREA}, genotypes of these groups were however recovered at the end point, indicating that they might still contribute to a smaller extent to hydrogen, and possibly acetate, consumption (Fig. 5, OTU5, OTU6).

At the end point of both R_{UREA} and R_{OLR}, an additional group of hydrogenotrophic methanogens appeared, representing about 9–10% of the partial *mcrA* genes obtained in the clone libraries. These clones, designated OTU3 and OTU4 (Fig. 5), were related to *Methanomassiliicoccaceae*. Members of this family have recently been described as obligate hydrogen-consuming methanogens, reducing methanol and methylamines instead of carbon dioxide (Dridi *et al.*, 2012). Thus, an additional methanogenic pathway might contribute to methane production at high OLR, as also recently concluded by Hori and colleagues for

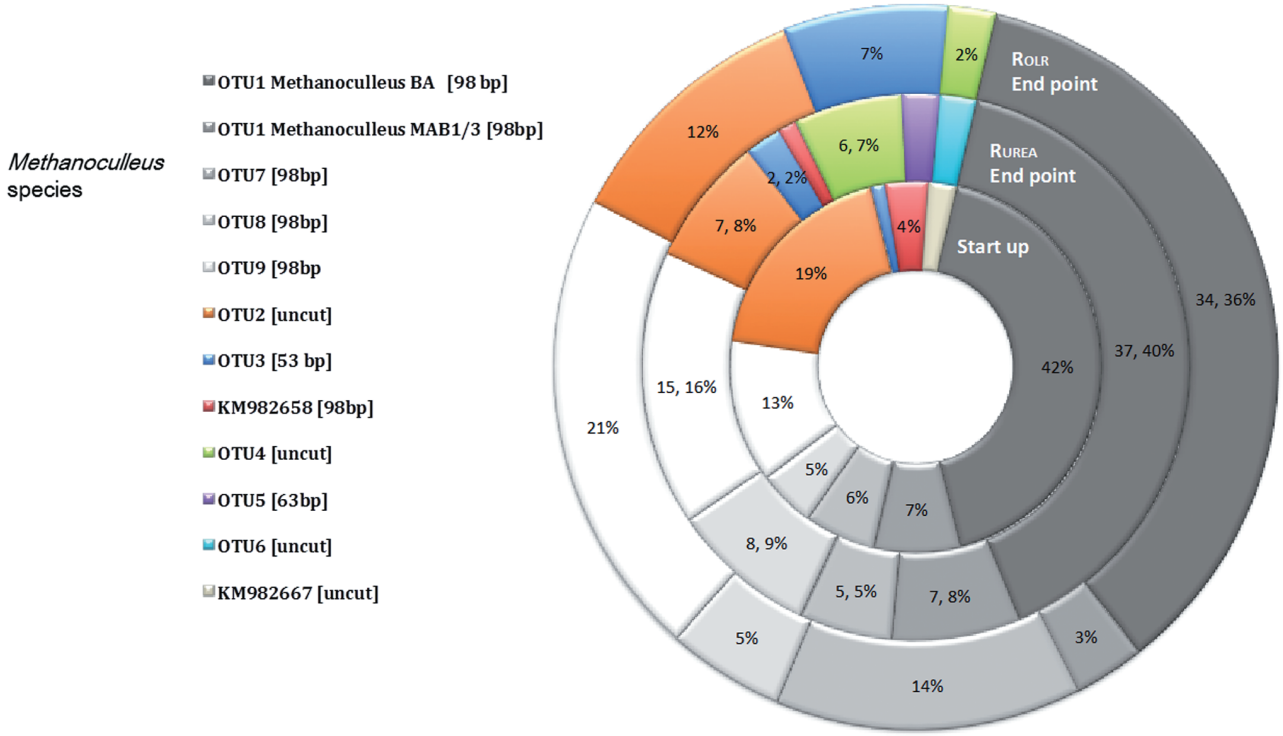

Fig. 5. Deeper analysis of the clone library, correlated to the T-RFLP analysis of the *mcrA* gene. Start-up represents reactor R_{OLR} at day 72 before any changes were made in the experiment. End point represents day 554 in R_{OLR} and day 583 in R_{UREA}.

thermophilic biogas processes (Borrel *et al.*, 2013; Hori *et al.*, 2014). Since only a small proportion of OTU3 was recovered from R_{UREA}, the appearance could be correlated to a likely higher availability of substrates as a consequence of higher OLR.

Acetogenic population analysis

Terminal restriction fragment length pattern analysis targeting the formyltetrahydrofolate synthetase (*fhs*) genes combined with clone libraries was conducted on start-up and at the end point, i.e. in the same samples as used for analysis of the methanogenic community (Fig. 6; Fig. 7). The T-RFLP pattern at start-up was similar for the two reactors and was mainly dominated by T-RFs 76, 187, 221, 264 and 391 (Fig. 6, blue). However, concurrently with increasing FAN, this initially dominant group clearly declined in abundance in both reactors (Fig. 6, blue). Instead, T-RFs 52, 73, 113, 161, 183 and 260, which were initially present at low relative abundance, increased at

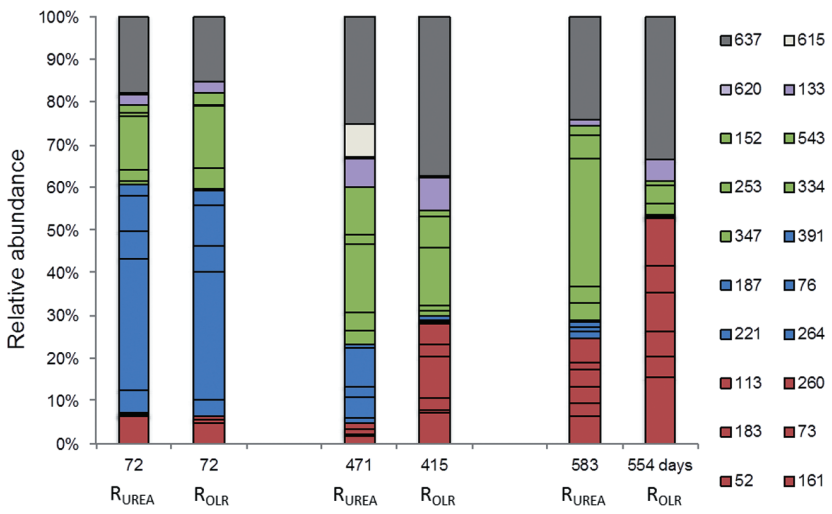

Fig. 6. Terminal restriction fragment length pattern analysis of acetogens. Fraction of relative abundance for all sequences with a limit of > 3% relative abundance. Red: enriched in both reactors (but faster and with higher abundance under increasing OLR conditions). Blue: fading in both reactors. Green: increasing under urea dosage conditions (but fading slowly with OLR). Light purple: same behaviour under both conditions. Light brown: single peak. Grey: uncut genotypes.

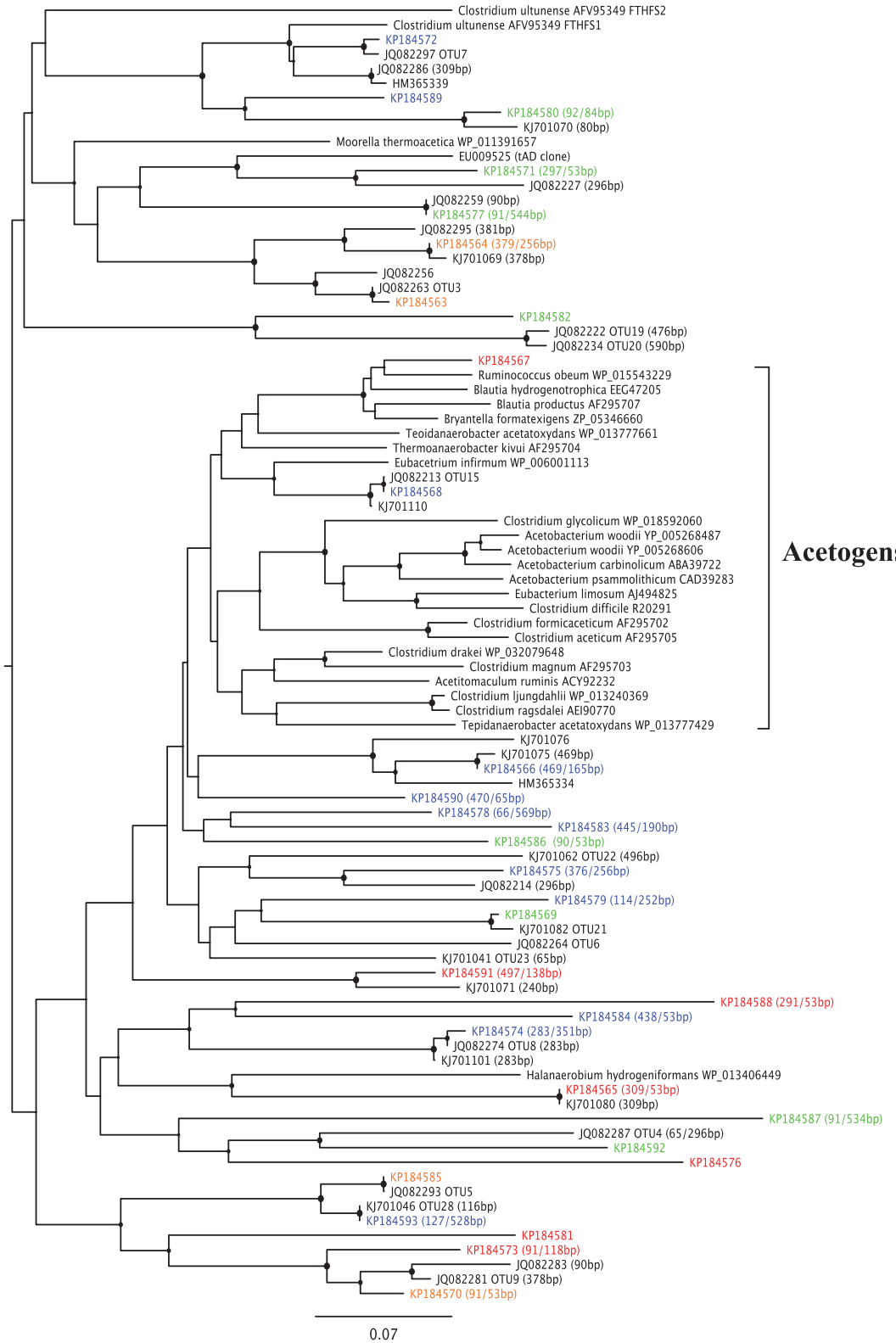

Fig. 7. Phylogenetic tree constructed of sequences retrieved in the clone library of the formyltetrahydrofolate synthetase (*fhs*) gene. Operational taxonomic units retrieved from three different samples (start-up and end point of each reactor). Start-up sample represents R_{OLR} at day 72 before any changes were made in the experiment. End point represents day 554 in R_{OLR} and day 583 in R_{UREA}. Blue group – fading from start-up; Orange group – detected in both end point clone libraries; Green group – only detected in R_{UREA} end point and Red group – only detected in R_{OLR} end point.

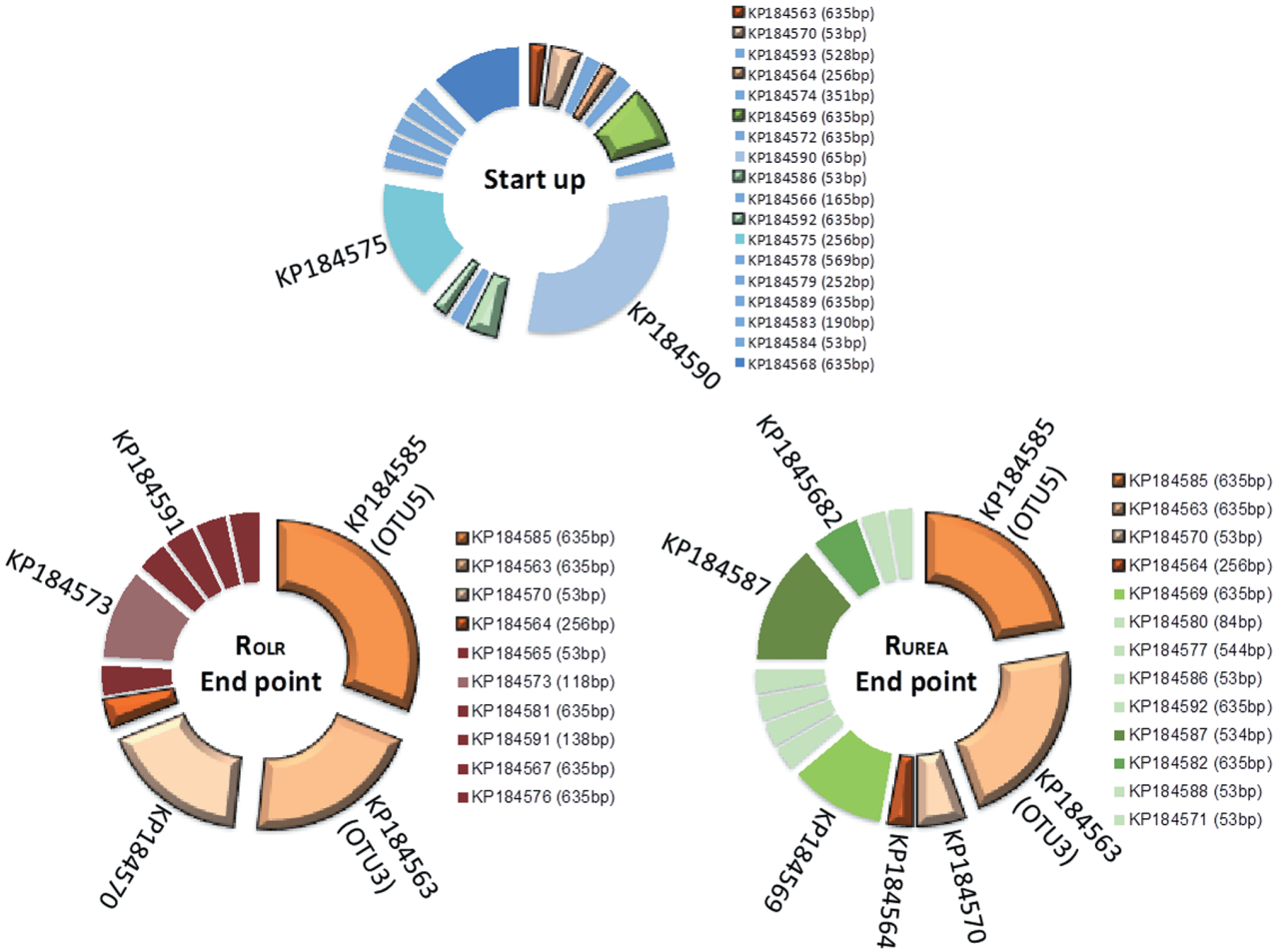

Fig. 8. Correlation between T-RFLP analysis and OTUs identified from clone libraries of the formyltetrahydrofolate synthetase (*fhs*) gene. Start-up sample represents R_{OLR} at day 72, before any changes were made in the experiment. End point represents day 554 in R_{OLR} and day 583 in R_{UREA}. Blue group – Fading from start-up; Orange group – detected in both end point clone libraries; Green group – only detected in R_{UREA} end point and Red group – only detected in R_{OLR} end point.

the last sampling point, with a higher presence in R_{OLR} compared with R_{UREA} (Fig. 6, red). Between start-up and end point, the total group (red) increased from 6% to 15% in R_{UREA} and 5% to 33% in R_{OLR}. Within the red group, T-RF 161 was the dominant T-RF, and the abundance increased from 4.5% up to 12.3% in R_{OLR}, whereas in R_{UREA}, this T-RF had almost the same abundance (5.6%) at the end point as observed at start-up.

Instead of the red group, which did not increase as much in R_{UREA} as in R_{OLR}, another group represented by T-RFs 152, 253, 334, 347 and 543 increased in R_{UREA} but slowly faded in R_{OLR} (Fig. 6, green group). A fourth group (Fig. 6, purple group), represented by T-RFs 133 and 620, was present at similar levels in both reactors over the whole operating period, obviously unaffected by increasing FAN and OLR.

The observed changes in the T-RFLP profiles were also reflected by the composition of the clone libraries. The majority of the genotypes recovered at the start-up point were not recovered at the end point (Fig. 8, blue group). About 28% and 47% of total number of clones obtained in the libraries were recovered uniquely from R_{OLR} or R_{UREA}, respectively (Fig. 8), indicating higher diversity in terms of number of OTUs in R_{UREA}. The recovered *fhs* genotypes were mainly distantly related to characterized acetogens (Fig. 7), as previously observed in other biogas systems (Westerholm *et al.*, 2011b). On correlating the results from the T-RFLP analysis with the clone libraries, most T-RFs could be identified. Among these, clones KP184590 and KP184575 were exclusively recovered from the start-up point and most likely correspond to T-RFs 76 and 264, which belonged to the blue group (Fig. 6) declining in both reactors in pace with the increasing ammonia level. In the phylogenetic tree, these clones separated from genotypes recovered from the end point and the higher FAN concentrations (Fig. 7). Despite the comparatively high initial FAN level in reactors R_{OLR} and R_{UREA}, KP184590 and KP184575 were closely related or identical to

genotypes previously found in low-FAN systems (Westerholm *et al*., 2011b; B. Müller, *et al*., unpublished).

Genotype KP184570 can probably be considered representative of T-RF 52 in the red group (Fig. 6) and KP184573 corresponded to T-RF 113 in the same group. In line with the results from the T-RFLP analysis, at the end point KP184570 was found at a higher frequency in the clone library of R_{OLR} than of R_{UREA}, and KP184573 was exclusively recovered form R_{OLR} (Fig. 8). Clone KP184591, possible corresponding to T-RF 133 (Fig. 6, purple), was also recovered exclusively from R_{OLR} but at low frequency. However, according to the T-RFLP analysis, this species appeared at similar but in general low abundances in both reactors in all sample points analysed. The abundance was slightly higher at the end point of R_{OLR} compared with the end point of R_{UREA}, which probably explains why it was only recovered from R_{OLR}. Thus, this species appeared rather stable and unaffected by both FAN and OLR dynamics in R_{OLR} and R_{UREA}.

The green T-RF group (Fig. 6) was represented by genotype KP184564, most likely corresponding to T-RF 253. This genotype was present in equal relative abundance in the clone libraries from the end point in both reactors and clustered in the phylogenetic tree (Fig. 7), together with clones previously recovered from a high FAN process (B. Müller, *et al*., unpublished). Another genotype belonging to the green group in the T-RFLP analysis was KP184587, corresponding to T-RF 543. This genotype grouped together with two additional genotypes recovered from R_{UREA} (KP184592 and KP184569) and one from R_{OLR} (KP184576) and were related to OTUs previously found to correlate with high ammonia processes (B. Müller, *et al*., unpublished). With a few exceptions, genotypes recovered exclusively from R_{UREA} (Fig. 7, green) did not group together with genotypes recovered exclusively from R_{OLR} (Fig. 7, red).

Between 13% and 27% of the relative abundance in both reactors (grey bars) remained uncut in the T-RFLP, this was due to lack of restriction sites (Fig. 6). From the clone library, the two most abundant genotypes in both reactor end points were represented within these uncut T-RFs. These two members (KP184563 and KP184585; orange in Fig. 8) were identical to OTUs found in a number of high-ammonia, laboratory-scale and large-scale reactors and suggested to be potential candidates for Syntrophic acetate oxidizing bacteria (SAOB) (B. Müller, *et al*., unpublished). In conclusion, the declining blue group (Fig. 6, Fig. 8) in the T-RFLP was mainly replaced by a core community consisting of KP184585, 63, 70, 64 and possible KP184573, in line with the increase in ammonia level (Fig. 8). In R_{OLR}, this core represented 72% of the *fhs* genotypes recovered (exclusive KP184573), compared with 53% in R_{UREA} (Fig. 8, orange), all representing genotypes potentially related to SAO (Fig. 7). Moreover, for both R_{OLR} and R_{UREA}, qPCR revealed a stable presence of the SAOB *Tepidanaerobacter acetatoxydans*, *Clostridium ultunense* and *Syntrophaceticus schinkii* (Fig. 9A) and the *fhs* OTUs 3, 4, 5, 7 and 9 (Fig. 9B), which all have been found in biogas processes operating at high FAN levels and which were partly recovered from the clone libraries (*fhs* OTU3 and OTU5). In both processes, the highest log-scaled gene copy numbers mL^{-1} (8.2–9.0) were achieved for *S. schinkii*, OTU 3 and OTU5 towards the end of the experiment with increasing FAN concentration. The log-scaled gene copy numbers/ml for *T. acetatoxydans*, *C. ultunense* (5.0–6.9) and OTUs 4, 7 (6.2–7.7) and 9 (4.8–6.6) were equally stable but lower, what likely explains their absence in the clone libraries. It is clear that the SAOB and the major part of the *fhs* OTUs analysed were prevailing in the reactors at these very high FAN levels, a result that support previous studies of high ammonia reactors (Westerholm *et al*., 2011b; Moestedt *et al*., 2014; Sun *et al*., 2014).

Furthermore, the changes observed in the T-RFLP analyses and clone library following increasing FAN concentration illustrate that the long adaptation period applied allowed enough time for changes in the acetogenic community. It is also quite clear that the T-RFs and genotypes belonging to the blue group (Fig. 6) were less tolerant to elevated FAN levels than the other groups. The difference of the community structure of the two reactors at elevated FAN could possibly explain the observed difference in VFA profile, with more propionate in R_{OLR}.

Terminal restriction fragment length pattern analyses performed on the acetogenic community in a process with increasing FAN concentration (from 0.03 to 0.24 g L^{-1}) have previously revealed two distinct shifts in the T-RFLP profile, indicating that the FAN concentration had a great effect on the composition of the acetogenic community and that an adaptation occurred in response to increasing levels (Westerholm and colleagues (2011b).

Despite the much lower FAN levels than in the present study, a comparable successive effect on the composition of the acetogenic population was observed. One effect observed here for both methanogens and acetogens was that the rise and fall in particular community members appeared to occur faster with the higher VFA throughput in R_{OLR}, probably forcing competition between groups able to treat the substrate.

Concluding remarks

The threshold concentration of FAN to maintain specific methane production in reactors treating thin stillage was determined to be 1.0–1.1 g L^{-1}, irrespective of OLR. Regardless of FAN level, the methanogenic community was dominated by hydrogenotrophic *Methanoculleus*-related species. However, different species within

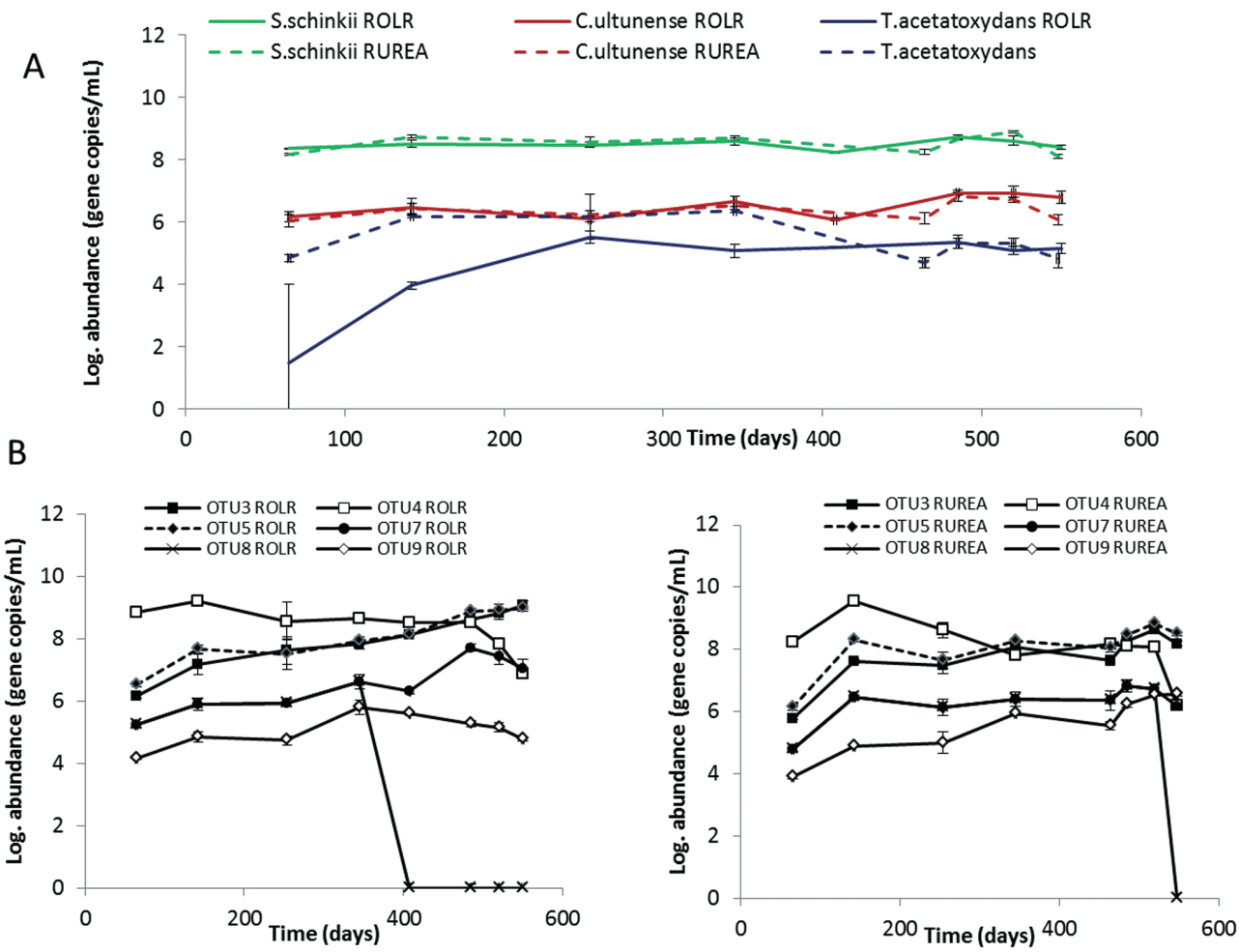

Fig. 9. Log abundance of known SAOB (A) and OTUs representing potential SAOB for R_{OLR} and R_{UREA} (B).

Methanoculleus dominated depending on the OLR. A different methanogenic pathway might contribute to methane production at high OLR, as indicated by the recovery of a potential representative from the hydrogenotrophic methanol-reducing *Methanomassiliicoccaceae*. As regards the acetogenic population, a distinct shift was observed when the FAN level was increased from 0.30 g L^{-1} to the threshold level (1.1 g L^{-1}), but the outcome differed depending on OLR. Several of the sequences retrieved from the process at high FAN levels clustered with genotypes previously found in other biogas processes operating at high FAN levels. With increasing OLR, the gene species diversity of the acetogenic population decreased and the composition of the community changed. At the threshold FAN concentration, the propionate level increased irrespective of OLR, indicating that propionate is a good indicator of FAN inhibition. Despite the difference in microbial populations, both reactors displayed process instability at a similar FAN level, suggesting that failure was caused by a general microbial ammonia inhibition threshold rather than limitations caused by overload.

Experimental procedures

Experimental set-up

Two 12-L CSTR (Tekniska verken i Linköping AB publ.) were operated for 574–653 days (Nordell *et al*., 2011). The active volume was 9 L, and the reactors were agitated continuously at 80 r.p.m. and fed semi-continuously (once a day) 7 days per week. Volume adjustment and sampling were performed 5 days per week, prior to daily feeding.

Inoculum was collected from a full-scale reactor (Tekniska verken i Linköping AB, Norrköping) and the OLR of VS during the 100-day start-up phase was 2.5 g L^{-1} d^{-1} thin stillage and 0.7 g L^{-1} d^{-1} milled grain. The thin stillage was obtained from a bio-ethanol plant (Lantmännen Agroetanol AB) in close proximity to the Norrköping biogas plant and frozen (–20°C). The milled grain was supplied by local farmers (Moestedt *et al*., 2013b). During the start-up period, process parameters and substrates in the laboratory-scale processes were kept

constant in order to mimic the conditions in the full-scale plant. Thus, temperature and HRT were set to 38°C and 45 days, respectively, and kept constant throughout the experiment. Tap water was used to dilute the thin stillage and the milled grain to reach the HRT of 45 days. After the start-up phase, from day 100, OLR was gradually increased in reactor R_{OLR}. To keep HRT constant, tap water was replaced by thin stillage to obtain the higher OLR, also resulting in a higher ingoing TAN concentration. In the other reactor (R_{UREA}) urea (Alfa Aesar GmbH, Germany) was added to the feedstock in order to increase the TAN concentration to the same level as the substrate to R_{OLR}, without increasing the loading. The increase in OLR and the urea dose are shown in Table 1. A third reactor (control) was started together with R_{OLR} and R_{UREA} with maintained conditions as used during start-up throughout the experimental time. This reactor maintained stable process and gas yield and ensured the quality of the results. The daily OLR was calculated as the VS weight fed into the reactor divided by the reactor volume plus feeding volume. A process additive containing iron (11%, a mixture of Fe^{2+}/Fe^{3+}), cobalt (18 mg kg^{-1}) and hydrochloric acid (< 0.5%) was used in both reactors, as in the full-scale plant (Ejlertsson, 2007; Moestedt *et al.*, 2013b). The additive was intended to suppress the H_2S concentration to 150 μL L^{-1} in the biogas and to keep the cobalt concentration at 0.5 mg L^{-1}. Volumetric gas production was measured online with a Ritter milligas counter (MGC-10, Ritter, Germany) and methane concentration with a gas sensor (BlueSens, Germany). Specific gas production was calculated as the amount of gas produced normalized on amount of organic material (measured as VS) added to the reactor per day. All volumetric gas data presented in this paper have been converted to standard conditions at pressure 1.01325 bar and temperature 273.2 K.

Chemical analyses

The VFA content was analysed with a Clarus 550 gas chromatograph (Perkin Elmer, USA) with a packed Elite-FFAP column (Perkin Elmer, USA) for acidic compounds according to Jonsson and Borén (2002). Ammonium nitrogen (TAN; NH_4-N) was analysed as the sum of NH_4–N (aq) + NH_3–N (aq) by distillation (Kjeltec 8200, FOSS in Scandinavia, Sweden) in an acidic solution (H_3BO_3) and NH_4-N was then determined by titration with HCl (Titro 809, Metrohm, Switzerland). Kjeldahl-nitrogen (kjel-N) was determined with the same procedure and equipment as NH_4-N, with the exception that the samples were pre-treated with H_2SO_4 and subsequently heated to 410°C for 1 h. The ammonia (FAN; NH_3-N) concentration was calculated from the NH_4-N concentration, pH and temperature according to Hansen and colleagues (1998b). pH was measured with a potentiometric pH meter at 25°C using a Hamilton electrode (WTW Inolab, USA). Dry matter (DM) was measured by oven drying at 105°C for 20 h, and VS was subsequently measured by combusting the DM sample at 550°C for 3 h.

Microbiological analyses

Quantitative PCR of methanogenic groups, SAOB and fhs OTUs

Methanogenic groups. Samples were withdrawn from the reactors, and deoxyribonucleic acid (DNA) was extracted in triplicate aliquots from each sample according to Moestedt and colleagues (2013a). Five sample points were used for qPCR, chosen to represent equal FAN concentrations in the two reactors. Samples were collected from R_{UREA} on days 72, 369, 471, 520 and 583, and from R_{OLR} on days 72, 310, 415, 513 and 554. Quantification was performed in triplicate using different dilutions (1:10, 1:50, 1:100) to observe and avoid inhibitory effects of the amplification reaction. Analysis of methanogenic groups (*Methanomicrobiales, Methanobacteriales, Methanosaetaceae* and *Methanosarcinaceae*) was performed according to protocols described elsewhere (Westerholm *et al.*, 2011a; Sun *et al.*, 2014), using IQ SYBR Green Supermix (Biorad, Herculas, CA). *SAOB and fhsOTUs*: Samples were retrieved as triplicates from days 65, 142, 254, 345, 408, 485, 520 and 550 in the case of R_{OLR} and 65, 142, 254, 345, 464, 485, 520 and 548 in the case of R_{UREA}, and purified as described in Moestedt and colleagues (2013b). Possible inhibition was excluded by comparing dilution series (1:10, 1:20) of OLR samples prior analyses. Finally, qPCR was performed using 1:20 dilutions according to the protocols described by Westerholm and colleagues (2011a) and (B. Müller, *et al.*, unpublished). Melt curve analysis and qPCR data processing were conducted as described previously (Moestedt *et al.*, 2013a), DNA was visualized by agarose gel-red Nucleic Acid (Biotium) electrophoresis using 1.5% agarose gels and 1 kb DNA ladder of Fermentas.

T-RFLP

Terminal restriction fragment length pattern analysis of the acetogenic and methanogenic communities was performed on triplicate sampling points, on days 72, 471 and 583 for R_{UREA} and days 72, 415 and 554 for R_{OLR}. The acetogenic community was recovered by the following touchdown PCR described by Müller and colleagues (2013) slightly modified: initial denaturation at 94°C for 5 min, followed by 11 cycles of denaturation at 94°C for 60 s, annealing at 63°C for 60 s (decreased by 1°C per cycle to 53°C) and elongation at 72°C for 60 s. Amplicons were enriched by 25 additional cycles conducted at 94°C for 60 s, 53°C for 60 s and 72°C for 60 s, finalized by 20 min at 72°C. The reaction consisted of 35 ng genomic DNA, 20 pmol each 3-SAO *fhs* primer (Müller *et al.*, 2013) and PuReTaq Ready-to-go PCR beads of GE Healthcare (Buckinghamshire, UK). The 3-SAO *fhs* reverse primer (Müller *et al.*, 2013) was labelled with 6-carboxyfluorescein (FAM). To reduce background noise, the respective bands at approximately 630 bp were gel purified using the QIAquick Gel Extraction Kit (Qiagen, Hilden, Germany) even though no unspecific bands were detectable. Deoxyribonucleic acid was visualized by agarose gel-red electrophoresis using 2% agarose gels and 1 kb DNA ladder of Fermentas. The methanogenic community was analysed by targeting the *mcrA* gene using the forward primer mlas and the FAM-labelled reverse primer mcrA-rev (Steinberg and Regan, 2008). The protocol used was: initial denaturation at 94°C for 3 min, followed by five cycles of denaturation at 94°C for 30 s, annealing at 48°C for 45 s (ramp rate 0.1°C/s) and elongation at 72°C for 30 s. Amplicons were enriched by 30 additional cycles conducted at 94°C for 30 s, 55°C for 45 s and 72°C for 30 s, finalized by 10 min at 72°C.

Terminal restriction fragments were obtained by subsequent digestion of the PCR products obtained, as

recommended by the manufacturer, with Hpy188III (Fermentas) and BstNI (Fermentas) for analysis of the acetogenic and methanogenic community respectively. Separation of T-RFs was performed by Uppsala Genome Center (Sweden) using the MapMarker 1000 (Rox) size standard and an ABI3730XL DNA analyser (Applied Biosystems). The fragment data obtained were analysed with Peak Scanner v1.0 software (Applied Biosystems). The resulting profiles were further evaluated in Excel (Microsoft, USA) setting the threshold value at 0.5% of total peak abundance.

Construction of clone libraries

In order to identify the dominant T-RFs, clone libraries were constructed from the three sampling points R_{OLR} day 72, 554 and R_{UREA} day 583 for both the acetogenic and methanogenic community. Polymerase chain reaction was conducted as described above from the triplicate DNA extractions using an unlabelled primer combination. The products were gel purified, pooled and cloned into the pGEMT vector system (Promega, Madison, WI USA) as recommended by the manufacturer. $CaCl_2$-competent *Escherichia coli* JM109 cells (Promega) were transformed by the ligation mixture according to the manufacturer's protocol. Clones with at least 94.5% identity on nucleotide level were considered as one OTU. The BLASTP search algorithm (National Library of Medicine) was used to identify the closest reference strain. Representatives from every OTU and single clones were deposited in GenBank with the following accession numbers (Table S1; Table S2). Methanogenic community: OTU1 (R_{OLR}554: KM982672-74, KM982676, KM982678, KM982681-85; R_{OLR}72: KM982655, KM982656, KM982658-62, KM982664-66, KM982668-69, KM982671; R_{UREA}583: KM982639-40, KM982644-47, KM982650-51), OTU2 (R_{UREA}583: KM982641, KM982643, KM982652; R_{OLR}72: KM982654, KM982657, KM982670), OTU3 (R_{OLR}554: KM982675, KM982677; R_{UREA}583: KM982649, R_{OLR}72: KM982663), OTU4 (R_{OLR}554: KM982679, R_{UREA}583 KM982637-38), OTU5 (R_{UREA}583: KM982653), OTU6 (R_{UREA}583: KM982648), R_{OLR}72 single clone KM982667. Acetogenic community: R_{OLR}72 (KP184564, KP184586, KP184592-93, KP184568, KP184572, KP184589-90, KP184566, KP184574-75, KP184578-79, KP184583-84), R_{OLR}554 (KP184563, KP184570, KP184565, KP184573, KP184581, KP184591, KP184567, KP184576), R_{UREA}583 (KP184569, KP184585, KP184580, KP184577, KP184587-88, KP184582, KP184571).

Tree construction

Multiple sequence alignments were performed using MAFFT v7.017 (Katoh *et al*., 2002) and maximum likelihood trees were constructed using PHYML v3.0 (Guidon and Gascuel, 2003), both implemented in GENEIOUS v6.1.8 (Biomatters. USA) including deduced amino acid sequence of partial *mcr*A respective *fhs* sequences affiliated to the accession numbers mentioned above, as well as reference strains. The *fhs* gene tree includes further partial *fhs*-gene sequences obtained by B. Müller, and colleagues (unpublished), Westerholm and colleagues (2011b) and Westerholm and colleagues (2015). Accession numbers are given in brackets.

Acknowledgements

Our thanks to Y. Calderon at Tekniska verken i Linköping AB (publ.), Simon Isaksson at the Swedish University of Agricultural Sciences for laboratory assistance and to Dr. Martin Karlsson at Linköping University for discussions about experimental design. The authors declare no conflict of interest.

Conflict of Interest

None declared.

References

Ahring, B.K., Sandberg, M., and Angelidaki, I. (1995) Volatile fatty-acids as indicators of process imbalance in anaerobic digesters. *Appl Microbiol Biotechnol* **43:** 559–565.

Angelidaki, I., and Ahring, B.K. (1993) Thermophilic anaerobic digestion of livestock waste: the effect of ammonia. *Appl Microbiol Biotechnol* **38:** 560–564.

Angelidaki, I., and Ahring, B.K. (1994) Anaerobic thermophilic digestion of manure at different ammonia loads – effect of temperature. *Water Res* **28:** 727–731.

Angelidaki, I., Karakashev, D., Batstone, D.J., Plugge, C.M., and Stams, A.J.M. (2011) Biomethanation and its potential. In *Methods in Enzymology: Methods in Methane Metabolism*. Rosenzweig, A.C., and Ragsdale, S.W. (eds). San Diego, USA: Elsevier Academic Press, pp. 327–351.

Angenent, L.T., Sung, S., and Raskin, L. (2002) Methanogenic population dynamics during startup of a full-scale anaerobic sequencing batch reactor treating swine waste. *Water Res* **36:** 4648–4654.

Borrel, G., O'Toole, P.W., Harris, H.M.B., Peyret, P., Brugère, J.-F., and Gribaldo, S. (2013) Phylogenomic data support a seventh order of methylotrophic methanogens and provide insights into the evolutions of Methanogenesis. *Genome Biol Evol* **5:** 1769–1780.

Calli, B., Mertoglu, B., Inanc, B., and Yenigun, O. (2005) Effects of high free ammonia concentrations on the performances of anaerobic bioreactors. *Process Biochem* **40:** 1285–1292.

Cardinali-Rezende, J., Colturato, L.F.D.B., Colturato, T.D.B., Chartone-Souza, E., Nascimento, A.M.A., and Sanz, J.L. (2012) Prokaryotic diversity and dynamics in a full-scale municipal solid waste anaerobic reactor from start-up to steady-state conditions. *Bioresour Technol* **119:** 373–383.

Chen, Y., Cheng, J.J., and Creamer, K.S. (2008) Inhibition of anaerobic digestion process: a review. *Bioresour Technol* **99:** 4044–4064.

Dridi, B., Fardeau, M.L., Ollivier, B., Raoult, D., and Drancourt, M. (2012) Methanomassiliicoccus luminyensis gen. nov., sp. nov., a methanogenic archaeon isolated from human faeces. *Int J Syst Evol Microbiol* **62:** 1902–1907.

Ejlertsson, J. (2007) United States Patent Application 20070184542.

Ek, A., Hallin, S., Vallin, L., Schnürer, A., and Karlsson, M. (2011) Slaughterhouse waste co-digestion – experiences from 15 years of full-scale operation. In: Proceedings of World Renewable Energy Congress. Linköping, Sweden.

Guidon, S., and Gascuel, O. (2003) A simple, fast, and accurate algorithm to estimate large phylogenies by maximum likelihood. *Syst Biol* **52:** 696–704.

Hansen, K.H., Angelidaki, I., and Ahring, B.K. (1998a) Anaerobic digestion of swine manure: inhibition by ammonia. *Water Res* **32:** 5–12.

Hansen, K.H., Angelidaki, I., and Ahring, B.K. (1998b) Anaerobic digestion of swine manure: inhibition by ammonia. *Water Res* **32:** 5–12.

Hori, T., Haruta, S., Sasaki, D., Hanajima, D., Ueno, Y., Ogata, A., *et al*. (2014) Reorganization of the bacterial and archaeal populations associated with organic loading conditions in a thermophilic anaerobic digester. *J Biosci Bioeng*.

Jonsson, S., and Borén, H. (2002) Analysis of mono- and diesters of o-phthalic acid by solid-phase extractions with polystyrene-divinylbenzene-based polymers. *J Chromatogr A* **963:** 393–400.

Karakashev, D., Batstone, D.J., Trably, E., and Angelidaki, I. (2006) Acetate oxidation is the dominant methanogenic pathway from acetate in the absence of Methanosaetaceae. *Appl Environ Microbiol* **72:** 5138–5141.

Katoh, K., Misawa, K., Kuma, K.-I., and Miyata, T. (2002) MAFFT: a novel method for rapid multiple sequence alignment based on fast Fourier transform. *Nucleic Acids Res* **30:** 3059–3066.

Koster, I.W., and Lettinga, G. (1984) The influence of ammonium-nitrogen on the specific activity of pelletized methanogenic sludge. *Agric Wastes* **9:** 205–216.

Lauterböck, B., Ortner, M., Haider, R., and Fuchs, W. (2012) Counteracting ammonia inhibition in anaerobic digestion by removal with a hollow fiber membrane contactor. *Water Res* **46:** 4861–4869.

Moestedt, J. (2015) Biogas production from thin stillage – exploring the microbial response to sulphate and ammonia. *Acta Universitatis Agriculturae Sueciae 2015:10 (Doctoral thesis)*. Uppsala, Sweden: Swedish University of Agricultural Sciences, p. 10.

Moestedt, J., Nilsson Påledal, S., and Schnürer, A. (2013a) The effect of substrate and operational parameters on the abundance of sulphate-reducing bacteria in industrial anaerobic biogas digesters. *Bioresour Technol* **132:** 327–332.

Moestedt, J., Nilsson Påledal, S., Schnürer, A., and Nordell, E. (2013b) Biogas production from thin stillage on an industrial scale – experience and optimization. *Energies* **6:** 5642–5655.

Moestedt, J., Nordell, E., and Schnürer, A. (2014) Comparison of operating strategies for increased biogas production from thin stillage. *J Biotechnol* **175:** 22–30.

Müller, B., Sun, L., and Schnürer, A. (2013) First insights into the syntrophic acetate-oxidizing bacteria – a genetic study. *Microbiologyopen* **2:** 35–53.

Nikolausz, M., Walter, R.F., Strauber, H., Liebetrau, J., Schmidt, T., Kleinsteuber, S., *et al*. (2013) Evaluation of stable isotope fingerprinting techniques for the assessment of the predominant methanogenic pathways in anaerobic digesters. *Appl Microbiol Biotechnol* **97:** 2251–2262.

Nordell, E., Moestedt, J., and Karlsson, M. (2011) Biogas Producing Laboratory Reactor, Application No. 1150954-4. SE.

Nordell, E., Hansson, A.B., and Karlsson, M. (2013) Zeolites relieves inhibitory stress from high concentrations of long chain fatty acids. *Waste Manag* **33:** 2659–2663.

Rajagopal, R., Massé, D.I., and Sing, G. (2013) A critical review on inhibition of anaerobic digestion process by excess ammonia. *Bioresour Technol* **143:** 632–641.

Schnürer, A., and Nordberg, A. (2008) Ammonia, a selective agent for methane production by syntrophic acetate oxidation at mesophilic temperature. *Water Sci Technol* **57:** 735–740.

Schnürer, A., Zeller, G., and Svensson, B.H. (1999) Mesophilic syntrophic acetate oxidation during methane formation in biogas reactors. *FEMS Microbiol Ecol* **29:** 250–261.

Sprott, G.D., and Patel, G.B. (1986) Ammonia toxicity in pure cultures of methanogenic bacteria. *Syst Appl Microbiol* **7:** 358–363.

Steinberg, L.M., and Regan, J.M. (2008) Phylogenetic comparison of the methanogenic communities from an acidic, oligotrophic fen and an anaerobic digester treating municipal wastewater sludge. *Appl Environ Microbiol* **74:** 6663–6671.

Sun, L., Müller, B., Westerholm, M., and Schnürer, A. (2014) Syntrophic acetate oxidation in industrial CSTR biogas digesters. *J Biotechnol* **171:** 39–44.

Werner, J.J., Garcia, M.L., Perkins, S.D., Yarasheski, K.E., Smith, S.R., Muegge, B., *et al*. (2014) Microbial community dynamics and stability during an ammonia-induced shift to syntrophic acetate oxidation. *Appl Environ Microbiol* **80:** 3375–3383.

Westerholm, M., Dolfing, J., Sherry, A., Gray, N.D., Head, I.M., and Schnurer, A. (2011a) Quantification of syntrophic acetate-oxidizing microbial communities in biogas processes. *Environ Microbiol Rep* **3:** 500–505.

Westerholm, M., Muller, B., Arthurson, V., and Schnurer, A. (2011b) Changes in the acetogenic population in a mesophilic anaerobic digester in response to increasing ammonia concentration. *Microbes Environ* **26:** 347–353.

Westerholm, M., Levén, L., and Schnurer, A. (2012) Bioargumentation of syntrophic acetate-oxidizing cultures in biogas reactors exposed to increasing levels of ammonia. *Appl Environ Microbiol* **78:** 7619–7625.

Westerholm, M., Müller, B., Isaksson, S., and Schnürer, A. (2015) Trace element and temperature effects on microbial communities and links to biogas digester performance at high ammonia levels. *Biotechnol Biofuels* **8:** 1–19.

Worm, P., Müller, N., Plugge, C.M., Stams, A.J.M., and Schink, B. (2010) Syntrophy in methanogenic degradation. In *(Endo)symbiotic Methanogenic Archaea*. Hackstein, J.H.P. (ed.). Heidelberg, Germany: Springer Berlin, pp. 149–173.

Yenigün, O., and Demirel, B. (2013) Ammonia inhibition in anaerobic digestion: a review. *Process Biochemistry* **48:** 901–911.

Zinder, S.H. (1984) Microbiology of anaerobic conversion of organic wastes to methane: recent developments. *ASM News* **50:** 294–298.

Zinder, S.H., and Koch, M. (1984) Non-aceticlastic methanogenesis from acetate: acetate oxidation by a thermophilic synthrophic coculture. *Arch Microbiol* **138:** 263–272.

Supporting information

Additional Supporting Information may be found in the online version of this article at the publisher's website:

Fig. S1. Terminal restriction fragment length pattern (T-RFLP) analysis of methanogens targeting the *mcrA* gene, with samples from reactor R_{OLR} and R_{UREA} sampled after 72, 471/415 and 583/584 days of operation. Fraction of relative abundance for all sequences > 1% relative abundance limit.

Table S1. Clones retrieved from reactor R_{OLR} at day 72 (ROLR72), assumed to illustrate start-up in both reactors, and from R_{OLR} at day 554 (R_{OLR}554) and R_{UREA} at day 583 (R_{UREA}583). Identities are based on nucleotide level. Accession numbers are also given.

Table S2. Summary of recovered partial formyltetrahydrofolate synthetase (fhs) genotypes. Clones retrieved from R_{OLR} at day 72 (R_{OLR}72) before the actual experiment started and from R_{OLR} at day 554 (R_{OLR} 554) and R_{UREA} at day 583 (R_{UREA} 583). Identities are based on nucleotide level. *In silico* restriction fragments are given both as 5'terminal fragment and 3'terminal fragment in order to compare with previous studies[1] (B. Müller, *et al.*, unpublished;[2] Westerholm *et al.*, 2015).

